Gas-Phase Fragmentation Pathways of Mixed Addenda Keggin Anions: PMo12-nWnO40 3- (n = 0-12)

ARTICLE *in* JOURNAL OF THE AMERICAN SOCIETY FOR MASS SPECTROMETRY · APRIL 2015

Impact Factor: 2.95 · DOI: 10.1007/s13361-015-1090-5 · Source: PubMed

J. Am. Soc. Mass Spectrom. (2015) 26:1027–1035
DOI: 10.1007/s13361-015-1090-5

RESEARCH ARTICLE

Gas-Phase Fragmentation Pathways of Mixed Addenda Keggin Anions: $PMo_{12-n}W_nO_{40}^{3-}$ (n = 0–12)

K. Don D. Gunaratne, Venkateshkumar Prabhakaran, Grant E. Johnson, Julia Laskin

Physical Sciences Division, Pacific Northwest National Laboratory, MSIN K8-88, P.O. Box 999, Richland, WA 99352, USA

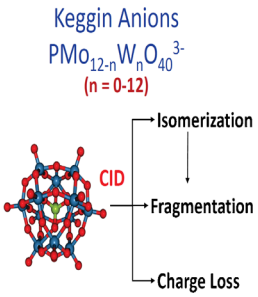

Abstract. We report a collision-induced dissociation (CID) investigation of the mixed addenda polyoxometalate (POM) anions, $PMo_{12-n}W_nO_{40}^{3-}$ (n = 0–12). The anions were generated in solution using a straightforward single-step synthesis approach and introduced into the gas phase by electrospray ionization (ESI). Distinct differences in fragmentation patterns were observed for the range of mixed addenda POMs examined in this study. CID of molybdenum-rich anions, $PMo_{12-n}W_nO_{40}^{3-}$ (n = 0–2), generates an abundant doubly charged fragment containing seven metal atoms (M) and 22 oxygen atoms ($M_7O_{22}^{2-}$) and its complementary singly charged $PM_5O_{18}^{-}$ ion. In comparison, the doubly charged Lindqvist anion, ($M_6O_{19}^{2-}$) and its complementary singly charged $PM_6O_{21}^{-}$ ion are the dominant fragments of Keggin POMs containing more than two tungsten atoms, $PMo_{12-n}W_nO_{40}^{3-}$ (n = 3–12). The observed transition in the dissociation pathways with an increase in the number of W atoms in the POM may be attributed to the higher barrier of tungsten-rich anions towards isomerization. We present evidence that the observed distribution of Mo and W atoms in the major $M_6O_{19}^{2-}$ and $M_7O_{22}^{2-}$ fragment ions is different from that predicted by a random distribution, indicating substantial segregation of the addenda metal atoms in the POMs. Charge reduction of the triply charged precursor anion resulting in formation of doubly charged anions is also observed. This is a dominant pathway for mixed POMs having a majority (8–11) of W atoms and a minor channel for other precursors indicating a close competition between fragmentation and charge loss pathways in CID of POM anions.

Keywords: Collision-induced dissociation, Anions, Mixed addenda Keggin, Polyoxometalate, Lindqvist, Isomerization, Electron detachment, Electrospray ionization

Received: 19 November 2014/Revised: 28 January 2015/Accepted: 28 January 2015/Published Online: 2 April 2015

Introduction

Polyoxometalates (POMs) are a class of inorganic materials that are of interest for a variety of applications because of their remarkable redox, photochemical, and magnetic properties [1–9]. The Keggin POM [10], a class of stable, redox-active, triply-charged anions comprised of a metal-oxide cage structure ($M_{12}O_{36}$; M = early transition metal) with an internal XO_4^{n-} group (typically X = Si, P; n = 4, 3, respectively), is one of the most widely studied POM systems. In POM nomenclature, the principal d-transition metal ions that form the molecular structural framework of POM in the MO_x coordination polyhedra are referred to as "addenda" atoms. The p-block elements at the center of the framework are referred to as "heteroatoms" [11]. The properties of Keggin-POMs may be tailored for a particular application by selecting the appropriate combination of transition metal addenda and internal heteroatoms.

The phosphomolybdates and phosphotungstates are two well-known Keggin species with the molecular formula $PM_{12}O_{40}^{3-}$, where M = Mo (Mo_{12}POM) and W (W_{12}POM), respectively. Although both the Mo_{12}POM and W_{12}POM demonstrate reversible, multi-electron redox activity, there are substantial differences between the properties of these two Keggin anions [1]. Specifically, W_{12}POM anions are more stable than the corresponding Mo_{12}POM species. Differences in the relative stability of Keggin POMs have been examined both experimentally and theoretically. The calculated bond lengths of the Keggin Mo_{12}POMs are generally longer than those of W_{12}POMs, indicating overall weaker bonds in the former [12, 13]. Comparison of the thermal stability between

Electronic supplementary material The online version of this article (doi:10.1007/s13361-015-1090-5) contains supplementary material, which is available to authorized users.

Correspondence to: Julia Laskin; *e-mail:* Julia.Laskin@pnnl.gov

$H_3PMo_{12}O_{40}$ and $H_3PW_{12}O_{40}$ also revealed that the phosphotungstate is more stable than the phosphomolybdate [14]. The Mo_{12}POM is known to undergo hydrolysis in aqueous solutions and requires stabilization by addition of organic solvent [1, 15]. In comparison, the W_{12}POM is stable in aqueous media [1]. In addition, the Mo_{12}POM readily forms protonated POMs via two-proton, two-electron reduction in acidic electrolyte solutions [16], whereas the W_{12}POM undergoes one-electron reductions without protonation at comparable conditions [17, 18]. The reduction potentials of Mo_{12}POM occur at more positive values compared with W_{12}POM, indicating that the former undergoes electrochemical reduction relatively easily [19]. Differences in redox properties of Mo_{12}POM and W_{12}POM stem from variations in the electronic structure of these two POMs. Specifically, the energy gap between the highest occupied molecular orbital and the lowest unoccupied molecular orbital (HOMO-LUMO gap) is estimated to be 2.0 eV for Mo_{12}POM and 2.8 eV for W_{12}POM [12]. Photoelectron spectroscopy experiments combined with density functional theory (DFT) calculations showed that the HOMO of W_{12}POM is stabilized by ~0.35 eV relative to that of Mo_{12}POM resulting in a corresponding increase in the vertical electron detachment energy from 1.94 eV for Mo_{12}POM to 2.30 eV for W_{12}POM [20].

Mixed addenda POMs have been examined previously by many research groups in an effort to access a range of electronic properties of interest to catalysis, energy storage, and chemical sensing [1, 2, 5, 11]. By changing the ratio of the transition metals, one may tailor the reactivity and stability of mixed addenda POMs for a particular application. For example, achieving a balance between reactivity and stability is important for catalyst materials that are widely used to improve the efficiency of chemical reactions. Specifically, a catalyst must bind reactants strongly enough that they become activated towards reaction but not so strongly that they cannot leave. In addition, a catalyst must be stable enough to promote a large number of reactions and not degrade over time [21, 22].

Mass spectrometry enables a systematic investigation of the structures and stabilities of mixed addenda POMs providing unique information on the effect of individual transition metal atoms on the properties of these species [9, 23]. Mixed Keggin POMs with Mo and W have been investigated previously by several research groups both theoretically [24] and experimentally [25, 26]. In the present study, we use a straightforward method of preparing mixed addenda Keggin POMs, $PMo_{12-n}W_nO_{40}^{3-}$ (n = 0–12), for analysis by electrospray ionization mass spectrometry (ESI-MS) and examine their dissociation pathways and relative stability towards fragmentation by means of collision-induced dissociation (CID) experiments. A few groups have previously studied the Keggin Mo_{12}POM, W_{12}POM, and selected mixed addenda POMs employing CID to analyze fragmentation patterns of the respective species [27–32]. However, to the best of our knowledge, there are no prior reports of systematic atom-by-atom CID studies of the full range of mixed addenda Keggin POMs.

The results presented herein demonstrate that the competition between isomerization, fragmentation, and charge reduction in the mixed addenda POMs is highly sensitive to the composition of the precursor anion. For example, a sharp transition in the fragmentation pathways attributed to the competition between isomerization and fragmentation was observed following replacement of only two Mo addenda atoms with W atoms in the Mo_{12}POM. Furthermore, CID results reveal an increase in the relative stability of the anion and a fine balance between dissociation and charge reduction with an increase in the number of W atoms in the anion. Our findings provide insight into how the substitution of individual addenda atoms in Keggin POMs may be employed to tune the reactivity and stability of these widely studied species.

Experimental

Sodium phosphomolybdate hydrate ($Na_3[PMo_{12}O_{40}].xH_2O$ CAS: 1313-30-0), sodium phosphotungstate hydrate ($Na_3[PW_{12}O_{40}].xH_2O$ CAS: 312696-30-3), and methanol were purchased from Sigma-Aldrich (St. Louis, MO, USA) and used as received.

Stock solutions of mixed addenda POMs were prepared by a one-pot synthesis adapted from Altenau et al. [33], where specific molar ratios of Mo_{12}-POM:W_{12}-POM (3:9, 6:6, 9:3) were added to warm (~60–70°C) deionized water and stirred for 30 min. The final mixed addenda POM stock solutions had a concentration of approximately 0.1 M and a pH of 1. Solutions for ESI-MS were prepared by diluting the 0.1 M mixed POM stock solutions to 100 μM in methanol.

ESI-MS analysis of the mixed addenda POM solutions was performed using a Bruker HCT-ultra ion trap mass spectrometer (Bruker Daltonics, Bremen, Germany) operated in the negative ion mode. Sample solutions were introduced into the ESI source at a flow rate of 120 μL/h using a syringe pump (KD Scientific, Holliston, MA, USA). Typical mass spectrometer conditions were as follows: capillary temperature, 150°C; high voltage capillary, 3 kV; capillary exit voltage, −60 V; skimmer, –15 V; octopole rf amplitude, 85 V; scan range, 100–3000*m/z*. Negatively charged ions were isolated (isolation width of 15*m/z*) and subjected to CID using helium as the inert neutral collision partner. CID experiments were conducted using the smart fragmentation option of the instrument, in which the excitation amplitude was varied throughout the experiment in a range of 30%–200% of the user-defined excitation amplitude. This approach provides a better coverage of both low- and high-energy dissociation pathways of the precursor ions in a single MS/MS experiment. In this study, the excitation amplitude was adjusted for each POM anion to reduce the relative abundance of the precursor ion to ~30%. Twenty scans were averaged for each spectrum presented in the figures.

Results and Discussion

ESI-MS Characterization of Mixed Addenda Keggin Anions

The full range of mixed addenda POMs was produced employing a straightforward method described in the "Experimental" section. The POMs examined in this study adhere to the molecular formula; $PMo_{12-n}W_nO_{40}^{3-}$ (n = 0–12). Scheme 1 shows the structure of the Mo_{12}POM ion reported in our previous study [34]. For simplicity, we will hereafter use the number of Mo and W atoms in the structure to represent the triply charged POM anions (e.g., $PMo_6W_6O_{40}^{3-}$ = Mo_6W_6POM). Each of the prepared solutions produces a range of mixed addenda POMs correlated with the molar ratio of Mo_{12}POM:W_{12}POM used. For example, the ESI mass spectrum of the solution prepared by mixing a 9:3 ratio of Mo_{12}POM:W_{12}POM produces POMs ranging from Mo_{12}POM to Mo_7W_5POM with the Mo_9W_3POM showing the highest abundance. Consequently, the full range of mixed POMs was obtained by preparing solutions with Mo_{12}POM:W_{12}POM molar ratios of 3:9, 6:6, and 9:3. An ESI mass spectrum obtained by mixing equal volumes of all three solutions is shown in Figure 1. The spectrum contains a complete series of $PMo_{12-n}W_nO_{40}^{3-}$ (n = 0–12) anions. In addition to the 3-charged POMs, the related 2- charged POMs are produced by ESI [34–36]. An ESI mass spectrum that includes both the 3- and 2- ions of all the POMs is shown in Figure S1 of the Supplementary Material.

CID of Mixed Addenda Polyoxometalates

Each of the triply charged, anionic, mixed addenda POM species, along with the pure Mo_{12}POM and W_{12}POM anions, underwent CID revealing the most stable dissociation products for each POM. The mass spectra of all the POMs that were subjected to CID are compiled in Figure 2. The major fragments observed for each of the POMs are listed in Table 1 for quick reference. In addition, a complete listing of all dissociation products and their complementary fragments, along with

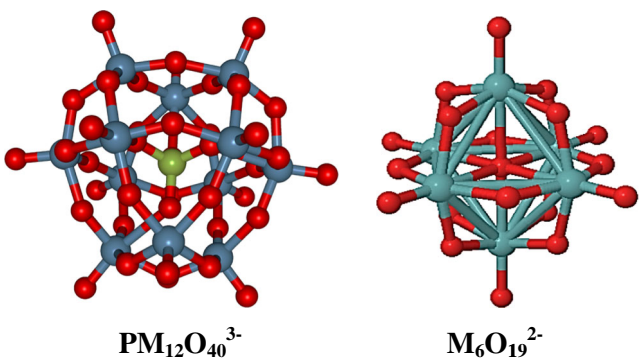

Scheme 1. Structures of the Keggin (left) and Lindqvist (right) anions

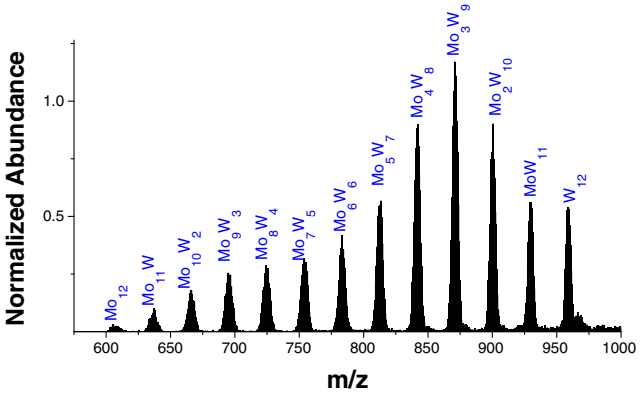

Figure 1. A representative mass spectrum obtained by electrospray ionization of the mixed addenda POM solutions. The observed POMs follow the stoichiometry; $PMo_{12-n}W_nO_{40}^{3-}$ (n = 0–12). The number of Mo and W atoms in each POM anion is provided in the peak labels

the normalized abundances of each product are provided in Table S1 of the Supplementary Material. Four types of major fragments were observed in the CID spectra and are color coded in Figure 2. CID of Mo_{12}POM, Mo_{11}WPOM, and $Mo_{10}W_2$POM primarily results in formation of $M_7O_{22}^{2-}$ and its complementary $PM_5O_{18}^{-}$ fragment (denoted in red in Figure 2) along with $M_8O_{25}^{2-}$ and its complementary $PM_4O_{15}^{-}$ fragment (denoted in green in Figure 2). In contrast, CID spectra of $PMo_{12-n}W_nO_{40}^{3-}$ (n = 3–12) anions are dominated by the Lindqvist anion $M_6O_{19}^{2-}$ shown in Scheme 1 and its complementary $PM_6O_{21}^{-}$ fragment (denoted in blue in Figure 2). The fourth type of fragments are color-coded purple in Figure 2 and correspond to the doubly charged POM anions produced either by electron detachment or protonation of the triply charged precursor POMs. The four major fragmentation pathways will be discussed in more detail in the next sections. Additionally, minor $M_3O_{10}^{2-}$, $M_4O_{13}^{2-}$, $M_5O_{16}^{2-}$, and $M_9O_{28}^{2-}$ fragments were observed as dissociation products but since their normalized abundances were well below 15% of the major fragments, they are not discussed in detail.

The fragmentation pathways of W_{12}POM and Mo_{12}POM observed in this study are consistent with the results reported previously by Ma et al. [31] for the W_{12}POM anion and by Cao et al. [32] for the Mo_{12}POM anion. Similar to these reports, we observe $M_6O_{19}^{2-}$ and $M_7O_{22}^{2-}$ as the major products of W_{12}POM and Mo_{12}POM, respectively. By varying the composition of the mixed addenda Keggin POMs, we were able to observe a transition from one major fragmentation pathway to another as shown in Figure 3. In the figure, the abundance of all $M_6O_{19}^{2-}$ and $M_7O_{22}^{2-}$ fragments normalized to the total intensity of CID fragments is plotted as a function of the number of tungsten atoms in the precursor ion. The inclusion of W atoms in the precursor POM anion results in an exponential decrease of the abundance of the $M_7O_{22}^{2-}$ fragment and a concomitant increase in the abundance of the $M_6O_{19}^{2-}$ fragment. The crossover point, at which both fragments are observed at almost

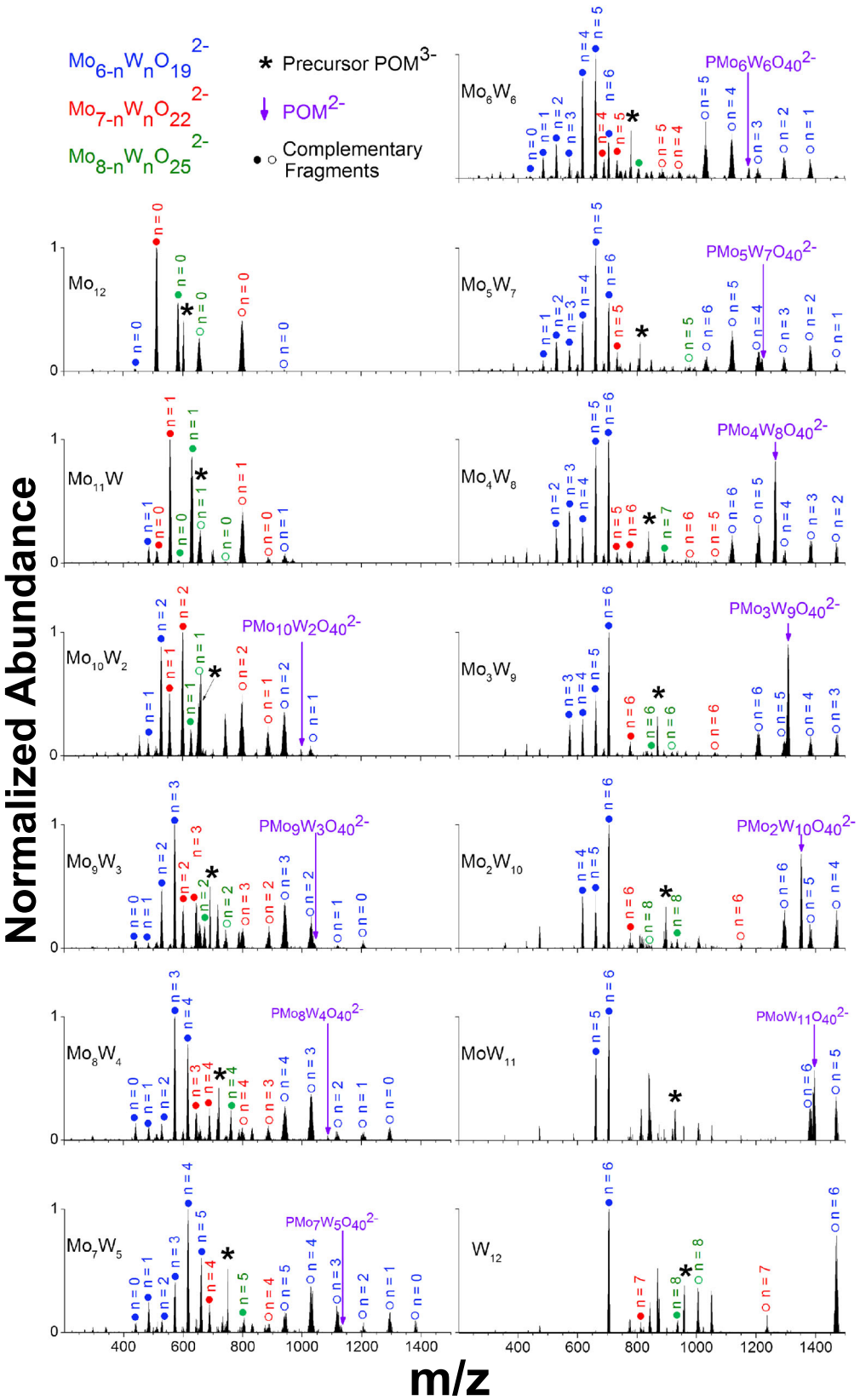

Figure 2. CID spectra of mass-selected mixed addenda polyoxometalates: $PMo_{12-n}W_nO_{40}^{3-}$ (n = 0–12). The precursor POMs are indicated by the 'star' symbol. The major metal-oxide doubly charged fragments are represented by color-coded filled circles; blue ($M_6O_{19}^{2-}$), red ($M_7O_{22}^{2-}$), and green ($M_8O_{25}^{2-}$), whereas their complementary fragments are denoted by unfilled circles of the same color. The charge loss products are indicated in purple

Table 1. The major CID products of each of the POM anions. The average *m/z* values for each peak are shown in parentheses

POM	Major Dissociation Products	
$PMo_{12}O_{40}^{3-}$ (607)	$Mo_7O_{22}^{2-}$ (512)	$PMo_5O_{18}^{-}$ (798)
$PMo_{11}WO_{40}^{3-}$ (637)	$Mo_6WO_{22}^{2-}$ (556)	$PMo_5O_{18}^{-}$ (798)
$PMo_{10}W_2O_{40}^{3-}$ (666)	$Mo_5W_2O_{22}^{2-}$ (600)	$PMo_5O_{18}^{-}$ (798)
$PMo_9W_3O_{40}^{3-}$ (695)	$Mo_3W_3O_{19}^{2-}$ (572)	$PMo_6O_{21}^{-}$ (942)
$PMo_8W_4O_{40}^{3-}$ (725)	$Mo_3W_3O_{19}^{2-}$ (572)	$PMo_5WO_{21}^{-}$ (1030)
$PMo_7W_5O_{40}^{3-}$ (754)	$Mo_2W_4O_{19}^{2-}$ (617)	$PMo_5WO_{21}^{-}$ (1030)
$PMo_6W_6O_{40}^{3-}$ (783)	$MoW_5O_{19}^{2-}$ (661)	$PMo_5WO_{21}^{-}$ (1030)
$PMo_5W_7O_{40}^{3-}$ (813)	$MoW_5O_{19}^{2-}$ (661)	$PMo_4W_2O_{21}^{-}$ (1118)
$PMo_4W_8O_{40}^{3-}$ (842)	$W_6O_{19}^{2-}$ (704)	$PMo_4W_2O_{21}^{-}$ (1118)
$PMo_3W_9O_{40}^{3-}$ (871)	$W_6O_{19}^{2-}$ (704)	$PMo_3W_3O_{21}^{-}$ (1206)
$PMo_2W_{10}O_{40}^{3-}$ (901)	$W_6O_{19}^{2-}$ (704)	$PMo_2W_4O_{21}^{-}$ (1294)
$PMoW_{11}O_{40}^{3-}$ (930)	$W_6O_{19}^{2-}$ (704)	$PMoW_5O_{21}^{-}$ (1383)
$PW_{12}O_{40}^{3-}$ (959)	$W_6O_{19}^{2-}$ (704)	$PW_6O_{19}^{-}$ (1471)

equal relative abundance, is observed when only two tungsten atoms are present in the POM. These results may be rationalized by assuming that either the structure of the precursor Keggin-POM or the energetics of the dissociation pathways are strongly affected by the addition of only one or two tungsten atoms to the molybdenum POM. The following discussion will address these questions in more detail.

Structural Isomers of Keggin Anions

The Keggin anions are known to have five structural isomers [37–39], which are formed by the 60° rotation of each of the four M_3O_{13} units of the lowest energy α-Keggin structure. It has been proposed that the α-Keggin isomer is the most stable as it has the least Coulomb repulsion between neighboring M–M units [40]. Indeed, as the Keggin structure changes from β, γ, δ, to the ε isomer, this M–M repulsion increases [39]. This also explains why, compared with the α and β isomers, the γ, δ, and ε structures are relatively unstable in the condensed phase. The γ isomers of select tungstates have previously been synthesized and isolated [41–44], and a few studies have

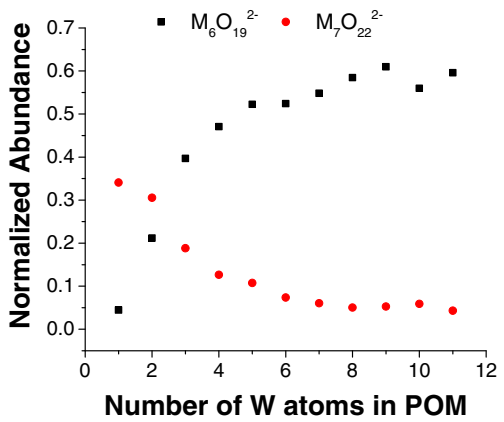

Figure 3. Evolution of the total abundance of $M_6O_{19}^{2-}$ versus $M_7O_{22}^{2-}$ dissociation products normalized to the signal of all CID fragments with an increasing number of W atoms in the mixed addenda POM. Range of POMs shown $Mo_{11}W$-MoW_{11}POM

reported the synthesis and characterization of ε-Keggin isomers with encapsulated ions [45–47].

Regarding the symmetry of these isomers, the α-Keggin has a structure with T_d symmetry, whereas the β-Keggin has C_{3v} symmetry [37, 48] The γ, δ, and ε Keggin anions belong to the symmetry groups C_{2v}, C_{3v}, and T_d, respectively [37]. It was also noted that the lowering of symmetry between the α and β forms did not have a substantial effect on the bonding in the unrotated M_3O_{13} units of the POM [48], although the same could not be said of the last three isomers. From the theoretical analysis performed on the γ-Keggin structure, the consensus is that the M–M bond distances are decreased to the point that a short M–M contact is formed in this isomer [37, 40, 49]. The number of M–M contacts was seen to increase to three and six for the δ and ε isomers, respectively [37]. Again, it is important to note that the instability of the latter three isomers is related to the Coulomb repulsion attributable to the decreased M–M distances of these Keggin structures. This may aid in explaining the CID fragmentation patterns we observed in this study.

For Mo_{12}POM and W_{12}POM anions, Poblet et al. [7] calculated the γ-Keggin isomer of W_{12}POM to be 13.9 kcal/mol (0.6 eV) higher in energy compared with the ground state α-Keggin structure, whereas for Mo_{12}POM, the γ-Keggin is estimated to be only 10.4 kcal/mol (0.45 eV) higher in energy. This 0.15 eV difference in energy between the α and γ isomers is large enough to be observed experimentally. We propose that the formation of the $M_7O_{22}^{2-}$ fragment may be attributed to the single close M–M contact, which is formed in the γ isomer as discussed in the literature. It is reasonable to propose that the Mo_{12}POM, Mo_{11}WPOM, and $Mo_{10}W_2$POM anions receive sufficient energy via multiple collisions that they form the γ-Keggin isomer with an additional M–M close contact, causing the preferential dissociation into the $M_7O_{22}^{2-}$ and its complementary fragment. The larger energy gap between α and γ isomers for tungsten-rich POM may inhibit isomerization into and fragmentation from the γ-Keggin structure. This likely explains the preferential formation of the $M_6O_{19}^{2-}$ Lindqvist anion, which is known to be the most abundant fragmentation product of the α isomer of W_{12}POM [31].

Stability of the Lindqvist Anion

The stability of the fragment ions may also be affected by the substitution of W for Mo in the precursor POM. To the best of our knowledge, the structure of the $M_7O_{22}^{2-}$ anion has not been discussed in the literature, whereas the $M_6O_{19}^{2-}$ Lindqvist anion has been studied both experimentally and theoretically [29, 30, 50–56]. Both $W_6O_{19}^{2-}$ and $Mo_6O_{19}^{2-}$ anions have been characterized using X-ray crystallography, which indicated that their structures are close to the ideal structure with the O_h symmetry [50, 51]. Photoelectron spectroscopy experiments by Yang et al. confirmed that despite the substantial intramolecular Coulomb repulsion both anions are very stable [56]. The somewhat higher adiabatic electron detachment energy of $W_6O_{19}^{2-}$ was attributed to the stronger metal–oxygen bonding in this system. These studies demonstrate that both the Mo- and W-based Lindqvist

anions are stable species, suggesting that the isomerization prior to fragmentation is likely the primary factor influencing the competition between the formation of $M_7O_{22}^{2-}$ and $M_6O_{19}^{2-}$ fragment ions in CID of the POM anions.

Segregation of Addenda Atoms in Mixed Addenda Keggin Anions

As expected, mixed addenda Keggin anions generate a distribution of $M_6O_{19}^{2-}$ and $M_7O_{22}^{2-}$ fragments and their complementary ions that contain both W and Mo atoms in different proportions. Assuming that metal atoms in the mixed addenda POM anions are randomly incorporated without segregation within the Keggin structure, the probability of removing a given number of W atoms, *r*, and Mo atoms, s, ($r + s = 6$ for $M_6O_{19}^{2-}$ and $r + s = 7$ for $M_7O_{22}^{2-}$) from *n* W atoms and (12-*n*) Mo atoms in the precursor anion is proportional to the number of combinations given by Equation 1:

$$C(n,r) = \frac{n!}{r!(n-r)!} \frac{12-n!}{s!(12-n-s)!} \quad (1)$$

The statistical probability distributions corresponding to random fragmentation of $PMo_{12-n}W_nO_{40}^{3-}$ anions were generated using Equation 1 and compared with the experimentally observed fragment distributions. The results of this comparison for the $M_6O_{19}^{2-}$ and $M_7O_{22}^{2-}$ fragments are shown in Figure 4. From inspection of this figure, it becomes evident that the experimental fragment distributions deviate substantially from the calculated random distributions. This deviation is more pronounced for the $M_6O_{19}^{2-}$ fragment (Figure 4a) and less pronounced for the $M_7O_{22}^{2-}$ fragment (Figure 4b). For all the precursor ions, we observe that the doubly charged $M_6O_{19}^{2-}$ and $M_7O_{22}^{2-}$ fragments are enriched with W atoms whereas Mo is preferentially partitioned into the complementary singly charged $PM_6O_{21}^{-}$ and $PM_5O_{18}^{-}$ fragments. Our results indicate that the metal atoms are not distributed randomly in the mixed addenda Keggin anions. This observation is consistent with previous results from the literature, which indicate that W atoms as well as other early transition metals substitute preferentially at the crown sites of mixed Keggin POMs [7, 24, 57, 58]. The formation of segregated islands of W within mixed addenda POMs may explain the non-statistical behavior presented in Figure 4. It is not clear why the $M_6O_{19}^{2-}$ and $M_7O_{22}^{2-}$ products are enriched in W instead of the complementary $PM_6O_{21}^{-}$ and $PM_5O_{18}^{-}$ fragments. It may possibly be attributed to the fact that W forms stronger bonds with oxygen than Mo atoms and, therefore, forms relatively more stable metal-oxide species than Mo.

Competition Between Fragmentation and Charge Loss

Another key observation made from the combined CID results presented in Figure 2 is the higher abundance of the doubly

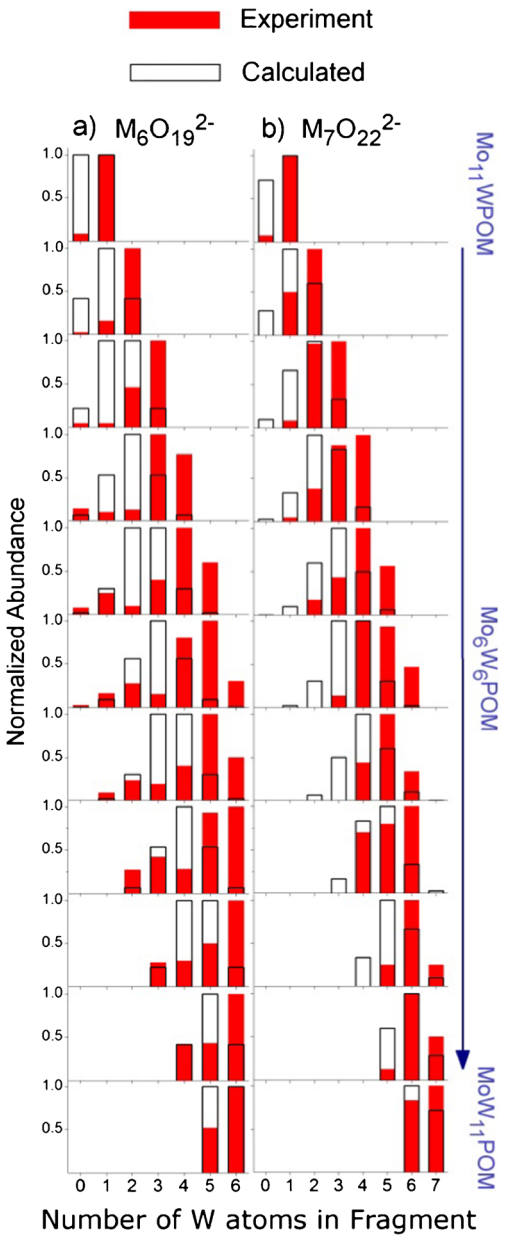

Figure 4. Comparison of the experimental abundances of the major fragments (red) with the calculated abundances of a purely statistical dissociation process (black outline). Columns (**a**) $M_6O_{19}^{2-}$ and (**b**) $M_7O_{22}^{2-}$ show the progression of these fragment abundances originating form collision induced dissociation of $Mo_{11}WPOM$ to $MoW_{11}POM$ (top to bottom)

charged POM anions with increasing amounts of W atoms in the mixed addenda Keggin system. The doubly charged POM is seen as a minor feature in the CID spectrum of $Mo_{10}W_2POM$ and it is present in all the mass spectra up to $MoW_{11}POM$. Interestingly, it is not present in the CID spectrum of $W_{12}POM$. As mentioned previously, the formation of the doubly charged mixed addenda POM may be attributed either to electron detachment or protonation of the triply charged precursor POM. It is not trivial to experimentally differentiate between electron loss and protonation by analyzing the mass spectra due

to the broad isotope distributions of both Mo and W. Regardless of the mechanism of charge loss, the competition between this pathway and fragmentation may aid in explaining the selective formation of doubly charged products of mixed addenda POMs containing 8–11 tungsten atoms. The energetics of these potential charge loss pathways is discussed below.

Electron loss from the triply charged precursor ion may occur either by direct electron detachment or a thermionic emission process [59]. In order for this process to efficiently compete with dissociation of the POM, the rate constant for electron detachment, determined by the electron binding energy, has to be close to the dissociation rate constant. Electron binding energies of 1.94 and 2.30 eV have been reported previously for the doubly charged Mo_{12}POM and W_{12}POM, respectively [20], whereas the HOMO-LUMO gaps for the triply charged anions are 2.03 and 2.8 eV for Mo_{12}POM and W_{12}POM, respectively [60]. These results indicate that regardless of the charge state, the electron binding energy of W_{12}POM is higher than that of Mo_{12}POM. In addition, Poblet and co-workers demonstrated that the energy of the LUMO is substantially decreased when only one W atom in the W_{12}POM is replaced with Mo [24]. It is reasonable to assume that the electron binding energies of the mixed addenda POMs described herein fall between these two extremes.

Protonation of the triply charged mixed addenda POMs may provide an alternate explanation for the doubly charged species observed in this study. Such a proton transfer process is possible depending on the proton affinities of the precursor POMs, presence of water molecules or other acidic neutral species in the mass spectrometer, and the residence time of the ions in the quadrupole ion trap. POMs are known to be basic species [1, 24] and previous studies have estimated the proton affinities of Mo_{12}POM and W_{12}POM to be 17.1 eV (394.3 kcal/mol) and 16.6 eV (382.8 kcal/mol), respectively [20, 61]. By comparison, the gas-phase acidity of water is in a range of 387.7–390.3 kcal/mol (http://webbook.nist.gov/chemistry/). It follows that proton transfer to Mo_{12}POM from water molecules in the bath gas of the ion trap is an exothermic process and may occur in our experiments. In contrast, proton transfer to W_{12}POM is endothermic and is unlikely to contribute to the observed charge loss. Although to the best of our knowledge proton affinities of mixed addenda Keggin POMs have not been calculated, it is reasonable to assume that the values for the $PMo_{12-n}W_nO_{40}^{3-}$ anions fall between the proton affinities of Mo_{12}POM and W_{12}POM. Since molybdenum-rich Keggin anions have higher proton affinities, one would expect to observe more efficient proton transfer with an increase in the number of Mo atoms. Instead, we observe the doubly charged mixed addenda POM only during CID of tungsten-rich $PMo_{12-n}W_nO_{40}^{3-}$ (n = 8–11) species while it is only a minor pathway for other precursor ions.

The lack of the charge loss product in the CID spectrum of W_{12}POM may be attributed to the relatively high electron binding energy and relatively low proton affinity of W_{12}POM, which suppress this pathway. In contrast, because of the lower electron binding energies and proton affinities of the mixed addenda POM examined in this study, charge loss from these precursor anions is more energetically favorable and may compete with fragmentation. The CID spectrum of Mo_{12}POM is dominated by other products, indicating that fragmentation of Mo_{12}POM is faster than the charge loss channel, whether it is by electron detachment or protonation.

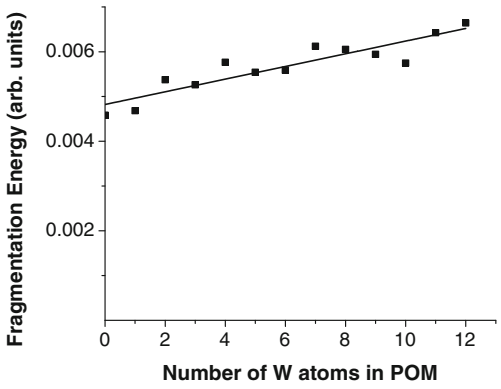

Figure 5. The increase of the effective center-of-mass energy required for the dissociation of the precursor POM ions with an increasing number of W atoms in the mixed addenda POM. The effective center-of-mass energy was calculated based on the excitation amplitude provided by the instrument software and is reported in arbitrary units

As discussed earlier, Mo_{12}POM is known to be less stable than W_{12}POM in solution. In order to explore the relative stability of the mixed addenda POM towards fragmentation in the gas phase, we examined the effect of the number of W atoms in the precursor ion on the effective center-of-mass fragmentation energy used in our CID experiments. The effective center-of-mass energy was calculated based on the excitation amplitude provided by the instrument software. The results are plotted in Figure 5. There is an obvious trend showing that the excitation energy required to observe a comparable amount of fragmentation increases with the number of W atoms in the POM anion. Similar trends were observed previously by Bonchio et al. during their experiments, which involved mixed POMs with vanadium and molybdenum atoms incorporated into the tungstate structure [28]. It follows that the charge loss process from Mo_{12}POM is not observed because of the lower dissociation thresholds. It appears that for the POMs consisting of 8–11 W atoms in the Keggin framework, both the fragmentation and charge loss pathways are characterized by similar rate constants, whereas fragmentation is the dominant process in CID of other POM anions. Our results indicate a close competition between fragmentation and charge loss pathways of mixed POM anions.

Conclusions

A straightforward single-step approach was used to prepare mixed addenda Keggin anions from Mo_{12}POM and W_{12}POM precursors in solution. The resulting $PMo_{12-n}W_nO_{40}^{3-}$ (n = 0–12) species were characterized using ESI-MS and CID. The CID results revealed the preference of

$Mo_{12}POM$, $Mo_{11}WPOM$, and $Mo_{10}W_2POM$ to form $M_7O_{22}^{2-}$ fragments (where M = a combination of Mo and W). In comparison, the well-known Lindqvist anion $M_6O_{19}^{2-}$ was observed as the major fragment of the other mixed addenda POM anions. The observation of $M_7O_{22}^{2-}$ species is attributed to the isomerization of $Mo_{12}POM$, $Mo_{11}WPOM$, and $Mo_{10}W_2POM$ into the γ-Keggin structure, which has one close M–M contact. The $PMo_{n-12}W_nO_{40}^{3-}$ (n = 3-12) anions, however, may not have isomerized beyond the α and β-Keggin structures.

The distribution of Mo and W atoms in $M_6O_{19}^{2-}$ and $M_7O_{22}^{2-}$ fragments observed experimentally were compared with the abundances for a purely statistical fragmentation process calculated assuming that the metal atoms are located randomly, without segregation, within the POM anions. It was found that the metal atoms do, in fact, segregate and prefer to form oxides involving more W atoms. This was attributed to the fact that W forms stronger metal–oxygen bonds compared to Mo.

During CID of mixed addenda POMs with a higher number of W atoms, apart from the dissociation products, charge loss products of the parent ions (i.e., the doubly-charged POMs) were also observed. Specifically, CID products of $PMo_{12-n}W_nO_{40}^{3-}$ (n = 8–11) showed an increased abundance of the doubly charged POMs, along with the other fragmentation products. This suggests that these mixed addenda POMs may have a close competition between fragmentation and charge loss. These results indicate that by choosing the type of transition metals and their combination, one may obtain mixed addenda POMs with a diverse range of structural and electronic properties. It also demonstrates that mass spectrometry is a powerful tool that provides atom-by-atom insight into how metal substitution in mixed addenda POMs influences their structure and stability.

Acknowledgments

The authors acknowledge support for this work by the U.S. Department of Energy (DOE) Office of Science, Office of Basic Energy Sciences, Division of Chemical Sciences, Geosciences, and Biosciences. This work was performed using EMSL, a national scientific user facility sponsored by the DOE's Office of Biological and Environmental Research and located at PNNL. PNNL is operated by Battelle for the U.S. DOE.

References

1. Sadakane, M., Steckhan, E.: Electrochemical properties of polyoxometalates as electrocatalysts. Chem. Rev. **98**, 219–238 (1998)
2. Katsoulis, D.E.: A survey of applications of polyoxometalates. Chem. Rev. **98**, 359–388 (1998)
3. Yamase, T.: Photo- and electrochromism of polyoxometalates and related materials. Chem. Rev. **98**, 307–326 (1998)
4. Song, Y.-F., Tsunashima, R.: Recent advances on polyoxometalate-based molecular and composite materials. Chem. Soc. Rev. **41**, 7384–7402 (2012)
5. Proust, A., Matt, B., Villanneau, R., Guillemot, G., Gouzerh, P., Izzet, G.: Functionalization and post-functionalization: a step towards polyoxometalate-based materials. Chem. Soc. Rev. **41**, 7605–7622 (2012)
6. Miras, H.N., Yan, J., Long, D.-L., Cronin, L.: Engineering polyoxometalates with emergent properties. Chem. Soc. Rev. **41**, 7403–7430 (2012)
7. Lopez, X., Carbo, J.J., Bo, C., Poblet, J.M.: Structure, properties, and reactivity of polyoxometalates: a theoretical perspective. Chem. Soc. Rev. **41**, 7537–7571 (2012)
8. Kourasi, M., Wills, R.G.A., Shah, A.A., Walsh, F.C.: Heteropolyacids for fuel cell applications. Electrochim. Acta **127**, 454–466 (2014)
9. Long, D.-L., Tsunashima, R., Cronin, L.: Polyoxometalates: building blocks for functional nanoscale systems. Angew. Chem. Int. Ed. **49**, 1736–1758 (2010)
10. Keggin, J.F.: The structure and formula of 12-phosphotungstic acid. Proc. R. Soc. London, Ser. A **144**, 75–100 (1934)
11. Hill, C.L., Prosser-McCartha, C.M.: Homogeneous catalysis by transition metal oxygen anion clusters. Coord. Chem. Rev. **143**, 407–455 (1995)
12. López, X., Maestre, J.M., Bo, C., Poblet, J.-M.: Electronic properties of polyoxometalates: a DFT study of α/β-$[XM_{12}O_{40}]^{n-}$ relative stability (M = W, Mo, and X a main group element). J. Am. Chem. Soc. **123**, 9571–9576 (2001)
13. Bridgeman, A.J.: Density functional study of the vibrational frequencies of α-Keggin heteropolyanions. Chem. Phys. **287**, 55–69 (2003)
14. Mizuno, N., Misono, M.: Heterogeneous catalysis. Chem. Rev. **98**, 199–218 (1998)
15. Papaconstantinou, E., Pope, M.T.: Heteropoly blues. III. Preparation and stabilities of reduced 18-molybdodiphosphates. Inorg. Chem. **6**, 1152–1155 (1967)
16. Barrows, J.N., Pope, M.T.: Intermolecular electron transfer and electron delocalization in molybdophosphate heteropoly anions. Adv. Chem. Ser. **226**, 403 (1990)
17. Keita, B., Nadjo, L.: New aspects of the electrochemistry of heteropolyacids: part IV. Acidity-dependent cyclic voltammetric behaviour of phosphotungstic and silicotungstic heteropolyanions in water and *N,N*-dimethylformamide. J. Electroanal. Chem. Interfacial Electrochem. **227**, 77–98 (1987)
18. Pope, M.T., Varga, G.M.: Heteropoly blues. I. Reduction stoichiometries and reduction potentials of some 12-tungstates. Inorg. Chem. **5**, 1249–1254 (1966)
19. Lewera, A., Chojak, M., Miecznikowski, K., Kulesza, P.J.: Identification and electroanalytical characterization of redox transitions in solid-state Keggin type phosphomolybdic acid. Electroanalysis **17**, 1471–1476 (2005)
20. Waters, T., Huang, X., Wang, X.-B., Woo, H.-K., O'Hair, R.A.J., Wedd, A.G., Wang, L.-S.: Photoelectron spectroscopy of free multiply charged Keggin anions α-$[PM_{12}O_{40}]^{3-}$ (M = Mo, W) in the gas phase. J. Phys. Chem. A **110**, 10737–10741 (2006)
21. Norskov, J.K., Bligaard, T., Hvolbaek, B., Abild-Pedersen, F., Chorkendorff, I., Christensen, C.H.: The nature of the active site in heterogeneous metal catalysis. Chem. Soc. Rev. **37**, 2163–2171 (2008)
22. Li, Y., Somorjai, G.A.: Nanoscale advances in catalysis and energy applications. Nano Lett. **10**, 2289–2295 (2010)
23. Miras, H.N., Wilson, E.F., Cronin, L.: Unravelling the complexities of inorganic and supramolecular self-assembly in solution with electrospray and cryospray mass spectrometry. Chem. Commun. **11**, 1297–1311 (2009)
24. López, X., Bo, C., Poblet, J.M.: Electronic properties of polyoxometalates: electron and proton affinity of mixed-addenda Keggin and Wells−Dawson Anions. J. Am. Chem. Soc. **124**, 12574–12582 (2002)
25. Deery, M.J., Howarth, O.W., Jennings, K.R.: Application of electrospray ionization mass spectrometry to the study of dilute aqueous oligomeric anions and their reactions. J. Chem. Soc. Dalton Trans. **24**, 4783–4788 (1997)
26. Williams, A.F.: Large coordination complexes: synthesis, characterization, and properties. Chem. Met. Alloys **2**, 1–9 (2009)
27. Cao, J., Xu, C., Fan, Y., Fan, L., Zhang, X., Hu, C.: Selective production of electrostatically-bound adducts of alkyl cations/polyoxoanions by the collision-induced fragmentations of their quaternary ammonium counterparts. J. Am. Soc. Mass Spectrom. **24**, 884–894 (2013)
28. Bonchio, M., Bortolini, O., Conte, V., Sartorel, A.: Electrospray behavior of lacunary Keggin-type polyoxotungstates $[XW_{11}O_{39}]^{p-}$ (X = Si, P): mass spectrometric evidence for a concentration-dependent incorporation of an MO^{n+} (M = W^{VI}, Mo^{VI}, V^{V}) unit into the polyoxometalate vacancy. Eur. J. Inorg. Chem. **2003**, 699–704 (2003)

29. Vilà-Nadal, L., Wilson, E.F., Miras, H.N., Rodríguez-Fortea, A., Cronin, L., Poblet, J.M.: Combined theoretical and mass spectrometry study of the formation-fragmentation of small polyoxomolybdates. Inorg. Chem. **50**, 7811–7819 (2011)
30. Lau, T.-C., Wang, J., Guevremont, R., Siu, K.W.M.: Electrospray tandem mass spectrometry of polyoxoanions. J. Chem. Soc. Chem. Commun. **8**, 877–878 (1995)
31. Ma, M.T., Waters, T., Beyer, K., Palamarczuk, R., Richardt, P.J.S., O'Hair, R.A.J., Wedd, A.G.: Gas-phase fragmentation of polyoxotungstate anions. Inorg. Chem. **48**, 598–606 (2008)
32. Cao, J., Li, C., Zhang, Z., Xu, C., Yan, J., Cui, F., Hu, C.: Intriguing role of a quaternary ammonium cation in the dissociation chemistry of keggin polyoxometalate anions. J. Am. Soc. Mass Spectrom. **23**, 366–374 (2012)
33. Altenau, J.J., Pope, M.T., Prados, R.A., So, H.: Models for heteropoly blues. Degrees of valence trapping in vanadium(IV)- and molybdenum(V)-substituted Keggin anions. Inorg. Chem. **14**, 417–421 (1975)
34. Gunaratne, K.D.D., Johnson, G.E., Andersen, A., Du, D., Zhang, W., Prabhakaran, V., Lin, Y., Laskin, J.: Controlling the charge state and redox properties of supported polyoxometalates via soft landing of mass-selected ions. J. Phys. Chem. C. **118**, 27611–27622 (2014)
35. Robbins, P.J., Surman, A.J., Thiel, J., Long, D.-L., Cronin, L.: Use of ion-mobility mass spectrometry (IMS-MS) to map polyoxometalate keplerate clusters and their supramolecular assemblies. Chem. Commun. **49**, 1909–1911 (2013)
36. Long, D.-L., Streb, C., Song, Y.-F., Mitchell, S., Cronin, L.: Unravelling the complexities of polyoxometalates in solution using mass spectrometry: protonation versus heteroatom inclusion. J. Am. Chem. Soc. **130**, 1830–1832 (2008)
37. López, X., Poblet, J.M.: DFT study on the five isomers of PW12O403–: relative stabilization upon reduction. Inorg. Chem. **43**, 6863–6865 (2004)
38. Pope, M.T.: Structural isomers of 1:12 and 2:18 heteropoly anions. Novel and unexpected chirality. Inorg. Chem. **15**, 2008–2010 (1976)
39. Baker, L.C.W., Figgis, J.S.: New fundamental type of inorganic complex: hybrid between heteropoly and conventional coordination complexes. Possibilities for geometrical isomerisms in 11-, 12-, 17-, and 18-heteropoly derivatives. J. Am. Chem. Soc. **92**, 3794–3797 (1970)
40. Kepert, D.L.: Structures of polyanions. Inorg. Chem. **8**, 1556–1558 (1969)
41. Cadot, E., Béreau, V., Marg, B., Halut, S., Sécheresse, F.: Syntheses and characterization of γ-$[SiW_{10}M_2S_2O_{38}]^{6-}$ (M = Mo^V, W^V). Two Keggin oxothio heteropolyanions with a metal−metal bond. Inorg. Chem. **35**, 3099–3106 (1996)
42. Zhang, X.-Y., O'Connor, C.J., Jameson, G.B., Pope, M.T.: High-valent manganese in polyoxotungstates. 3. dimanganese complexes of γ-Keggin anions. Inorg. Chem. **35**, 30–34 (1996)
43. Téazéa, A., Hervéa, G., Finke, R.G., Lyon, D.K.: α-, β-, and γ-Dodecatungstosilicic acids: isomers and related lacunary compounds. In: Inorganic synthesis, pp. 85–96. John Wiley and Sons, Inc., Hoboken (2007)
44. Uehara, K., Miyachi, T., Nakajima, T., Mizuno, N.: Effects of heteroatoms on electronic states of divanadium-substituted γ-Keggin-type polyoxometalates. Inorg. Chem. **53**, 3907–3918 (2014)
45. Khan, M.I., Müller, A., Dillinger, S., Bögge, H., Chen, Q., Zubieta, J.: Cation inclusion within the mixed-valence polyanion cluster $[(Mo^{V1}O_3)_4Mo_{12}VO_{28}(OH)_{12}]^{8-}$: syntheses and structures of $(NH_4)_7[NaMo_{16}(OH)_{12}O_{40}]\cdot 4H_2O$ and $(Me_2NH_2)_6[H_2Mo_{16}(OH)_{12}O_{40}]$. Angew. Chem. Int. Ed. **32**, 1780–1782 (1993)
46. Müller, A., Beugholt, C., Kögerler, P., Bögge, H., Bud'ko, S., Luban, M.: $[Mo^V_{12}O_{30}(\mu_2\text{-}OH)_{10}H_2\{Ni^{II}(H_2O)_3\}_4]$, a highly symmetrical ε-Keggin unit capped with four Ni^{II} centers:synthesis and magnetism. Inorg. Chem. **39**, 5176–5177 (2000)
47. Dolbecq, A., Mialane, P., Lisnard, L., Marrot, J., Sécheresse, F.: Hybrid organic–inorganic 1D and 2D frameworks with ε-Keggin polyoxomolybdates as building blocks. Chem. Eur. J. **9**, 2914–2920 (2003)
48. Bridgeman, A.J.: Computational study of the vibrational spectra of α- and β-Keggin polyoxometalates. Chem. Eur. J. **10**, 2935–2941 (2004)
49. Rohmer, M.-M., Benard, M.: Bond-stretch isomerism in strained inorganic molecules and in transition metal complexes: a revival? Chem. Soc. Rev. **30**, 340–354 (2001)
50. Fuchs, J., Freiwald, W., Hartl, H.: Crystal-structure of tetrabutylammoniumhexatungstate determined by difference Fourier methods. Acta Crystallogr., Sect. B: Struct. Sci. **34**, 1764–1770 (1978)
51. Clegg, W., Sheldrick, G.M., Garner, C.D., Walton, I.B.: Structure of bis(tetraphenylarsonium) hexamolybdate(VI). Acta Crystallogr., Sect. B: Struct. Sci. **38**, 2906–2909 (1982)
52. Rocchiccioli-Deltcheff, C., Fournier, M., Franck, R., Thouvenot, R.: Vibrational investigations of polyoxometalates. 2. Evidence for anion–anion interactions in molybdenum(VI) and tungsten(VI) compounds related to the Keggin structure. Inorg. Chem. **22**, 207–216 (1983)
53. Walanda, D.K., Burns, R.C., Lawrance, G.A., von Nagy-Felsobuki, E.I.: Electrospray mass spectral study of isopolyoxomolybdates. J. Chem. Soc., Dalton Trans. **3**, 311–322 (1999)
54. Walanda, D.K., Burns, R.C., Lawrance, G.A., von Nagy-Felsobuki, E.I.: Electrospray mass spectrometry of aqueous solutions of isopolyoxotungstates. J. Cluster Sci. **11**, 5–28 (2000)
55. Bridgeman, A.J., Cavigliasso, G.: Density functional study of the vibrational frequencies of lindqvist polyanions. Chem. Phys. **279**, 143–159 (2002)
56. Yang, X., Waters, T., Wang, X.-B., O'Hair, R.A.J., Wedd, A.G., Li, J., Dixon, D.A., Wang, L.-S.: Photoelectron spectroscopy of free polyoxoanions $Mo_6O_{19}^{2-}$ and $W_6O_{19}^{2-}$ in the gas phase. J. Phys. Chem. A **108**, 10089–10093 (2004)
57. Friedl, J., Al-Oweini, R., Herpich, M., Keita, B., Kortz, U., Stimming, U.: Electrochemical studies of tri-manganese substituted Keggin polyoxoanions. Electrochim. Acta **141**, 357–366 (2014)
58. Watras, M.J., Teplyakov, A.V.: Infrared and computational investigation of vanadium-substituted Keggin $[PV_nW_{12-n}O_{40}]^{(n+3)-}$ polyoxometallic anions. J. Phys. Chem. B **109**, 8928–8934 (2005)
59. Campbell, E.E.B., Levine, R.D.: Delayed ionization and fragmentation en route to thermionic emission: statistics and dynamics. Annu. Rev. Phys. Chem. **51**, 65–98 (2000)
60. Maestre, J.M., Lopez, X., Bo, C., Poblet, J.-M., Casañ-Pastor, N.: Electronic and magnetic properties of α-Keggin anions: A DFT study of $[XM_{12}O_{40}]^{n-}$, (M = W, Mo; X = Al^{III}, Si^{IV}, P^V, Fe^{III}, Co^{II}, Co^{III}) and $[SiM_{11}VO_{40}]^{m-}$ (M = Mo and W). J. Am. Chem. Soc. **123**, 3749–3758 (2001)
61. Ganapathy, S., Fournier, M., Paul, J.F., Delevoye, L., Guelton, M., Amoureux, J.P.: Location of protons in anhydrous Keggin heteropolyacids $H_3PMo_{12}O_{40}$ and $H_3PW_{12}O_{40}$ by $^1H\{^{31}P\}/^{31}P\{^1H\}$ REDOR NMR and DFT quantum chemical calculations. J. Am. Chem. Soc. **124**, 7821–7828 (2002)